Tellus (1994), 46B, 1–15
Printed in Belgium – all rights reserved

TELLUS
ISSN 0280–6509

The $(NH_4)_2SO_4$-Na_2SO_4-H_2O system: comparison of deliquescence humidities measured in the field and estimated from laboratory measurements and thermodynamic modeling

By SOTIRIA KOLOUTSOU-VAKAKIS and MARK J. ROOD*, *Environmental Engineering and Science Program, Department of Civil Engineering, University of Illinois at Urbana-Champaign, 205 N. Mathews, Urbana, IL 61801, USA*

(Manuscript received 26 January 1993; in final form 26 July 1993)

ABSTRACT

Hygroscopicity of atmospheric aerosol particles results in changes of the optical properties and chemical composition of the particles with significant effects on visibility degradation, atmospheric chemistry and possibly the global energy balance. Ambient aerosol, sampled in Riverside, California, USA, was characterized by measuring its light scattering coefficient as a function of controlled relative humidity and thermal treatment. These measurements and results from simultaneous filter samples have been compared with data from laboratory measurements and thermodynamic models for the $(NH_4)_2SO_4$-Na_2SO_4-H_2O system. Results from field experiments have indicated deliquescence humidities in the 74–79% range, after chemically neutralizing the aerosol with NH_3 and preheating the sample to 190°C. Preheating was used to remove more volatile material from the aerosol particles, such as NH_4NO_3 which could inhibit the occurrence of deliquescence. The measured deliquescence humidity values were less than expected for pure $(NH_4)_2SO_4$, but their mean is, at the 95% confidence level, the same with the means of predictions for the deliquescence humidities determined from the phase diagram and thermodynamic modeling for the $(NH_4)_2SO_4$-Na_2SO_4-H_2O system. These results indicate first the importance of mixtures when examining the hygroscopic characteristics of atmospheric aerosol particles, and second the usefulness of in situ optical methods for the assessment of the chemical composition and hygroscopic properties of atmospheric aerosols.

1. Introduction

The properties and effects of atmospheric aerosol particles depend on their physical state and chemical composition. Accurate characterization of the physics and chemistry of atmospheric aerosol is difficult, because of the complexity of the physical and chemical processes atmospheric aerosols experience and the large number of factors involved in these processes. The chemical composition of atmospheric aerosols can be inferred from measurements of their elemental or ionic composition as well as, from assessment of their physical and chemical behavior under carefully controlled conditions. For that to be possible, it is important to establish the relationships between observed behavior and chemical composition by comparing field data with laboratory observations and theoretical predictions. This paper presents the results of an effort in this direction, by using optical in situ field measurements and simultaneous filter measurements. The in situ optical measurements are compared with predictions from thermodynamic models based on results from the filter samples.

A common procedure for assessing the composition of aerosols is the collection of aerosol particles

* Corresponding author.

on a filter or impactor surface. One of the limitations of these methods is that it is difficult to say if an ion was originally present as a solid or in an aqueous solution. However, such information can be inferred by measuring deliquescence humidities and evaluating ambient relative humidity and aerosol composition histories of the aerosol sample. Therefore, it is useful to devise methods that would complement filter or impactor sampling, by allowing in situ observation of ambient aerosols and the changes the aerosols experience in conditions as close to their ambient environment as possible. Optical methods are appropriate for such purpose given the existing strong evidence that optical properties of the atmosphere are interlinked with the temporal and spatial variation of the chemical composition, mass concentration and particle-size distribution of aerosol particles (Charlson, 1969; Covert et al., 1972; Charlson et al., 1974; Covert et al., 1979; Tang et al., 1981; Sloane, 1986). Therefore, data collected with filters and/or impactors and data collected with optical methods can be used in a complementary way to investigate the chemistry, as well as the dynamics of ambient aerosols.

In this paper, changes of the aerosol light scattering coefficient, σ_{sp}, due to hygroscopicity and deliquescence are combined with filter data, laboratory measurements and thermodynamic modeling to assess the most likely chemical form of ions that predominated the ambient aerosol. The potential for in situ optical methods to make such an assessment is demonstrated. Detailed information about specific aerosol components is also provided, that can be included in a wider atmospheric modeling framework.

2. Sulfates and implications of their hygroscopicity in the atmosphere

Observations over different locations on the globe show that the major species in the overall aerosol mass are SO_4^{2-}, NO_3^-, NH_4^+, carbonaceous material, $H_2O_{(liquid)}$ and traces of alkalis and metals (Heintzenberg, 1989). Among these, SO_4^{2-} containing salts are the most common and comprise 28% of the mass of urban, 37% of the mass of non-urban continental and 22% of the mass of marine aerosols. SO_4^{2-} and NO_3^- salts are significant contributors to visibility reduction (Charlson et al., 1974; Covert et al., 1979; Cass, 1979). Their effect on visibility is related to aerosol particle size ($0.1 < d_p < 2\ \mu m$) which is in the same order of magnitude as the wavelength of visible light.

SO_4^{2-}, that is of interest in this paper, can exist as an acid or as a salt. $NH_{3(gas)}$ concentration and gas to particle conversion rates can determine the degree of chemical neutralization of SO_4^{2-} (Spann and Richardson, 1985). The possible NH_4^+ and SO_4^{2-} species are H_2SO_4, $(NH_4)HSO_4$, $(NH_4)_3H(SO_4)_2$, and $(NH_4)_2SO_4$. SO_4^{2-} containing salts are known to deliquesce when exposed to a moist environment. Deliquescence involves the abrupt phase transition from a solid particle to a saturated aqueous droplet when the relative humidity reaches a certain value, called deliquescence humidity. The deliquescence humidity corresponds to the water activity, α_w, of the saturated solution.

The interactions of H_2O with particles depend on the chemical nature of the particles. For example, H_2SO_4 absorbs $H_2O_{(gas)}$ monotonically with increasing $H_2O_{(gas)}$ concentration but when sufficient NH_3 exists in the atmosphere, to neutralize H_2SO_4 aerosol to $(NH_4)_2SO_4$, the aerosol particles can deliquesce at a relative humidity of about 80%. Deliquescence displays itself as a step change in the mass or σ_{sp} value of the aerosol. Therefore, measurement of σ_{sp} with and without $NH_{3(gas)}$ injection can classify the aerosol as largely $H_2SO_4/(NH_4)HSO_4$ or as $(NH_4)_2SO_4$ depending on the way the aerosol responds to increasing relative humidity conditions (Covert et al., 1972; Waggoner et al., 1981).

Single salt droplet growth has been studied experimentally and explained theoretically on the basis of thermodynamics (Orr et al., 1958; Tang, 1976). However, the growth of atmospheric aerosol particles is more complicated than explained by the single salt studies. In the atmosphere, changes in humidity and changes in chemical composition occur simultaneously. For example, due to dissolution of H_2O soluble gases, changes in relative humidity will result in changes of the concentration of solute in the aerosol droplets, pH and subsequently, in further chemical reactions, like dissociation of dissolved organic acids (Winkler, 1988). In addition, a solid salt mixture may go through several multiphase equilibria before the particle forms a homogeneous droplet. Deliquescence for a mixture of soluble components has experimentally been shown to

occur at a relative humidity lower than the one corresponding to any pure component (Rood et al., 1987a and b). The thermodynamic basis for this fact has also been provided (Wexler and Seinfeld, 1991).

Thermodynamic modeling predicts one step change regardless of the degree of mixing of the aerosol particle (Wexler and Seinfeld, 1991). That point corresponds to the "Mutual Deliquescence Humidity" of the mixture. At this point, there is the possibility of co-existence of a highly concentrated solution with one or more soluble solids in the droplet depending on the state of mixing of the aerosol particle. As relative humidity increases above the "Mutual Deliquescence Humidity", the soluble solid phases dissolve until a homogeneous droplet is formed that contains no solid soluble material. Semi-empirical models of this process have been presented in the literature (Hänel, 1976; Sloane, 1986). However, according to Wexler and Seinfeld (1991) not each point where a single component dissolves completely corresponds to a step change in mass. Nevertheless, step changes can occur (Tang et al., 1981; Rood et al., 1987a) because of hysteresis or nucleation events, which cannot be predicted by equilibrium thermodynamics.

3. Experimental procedure and results of field measurements

Field results used in this paper come from atmospheric aerosol sampling in Riverside, California, USA, between the 12 and 17 of September, 1983. The experimental procedure has been described previously (Rood et al., 1985; 1987a, b). A brief description of the procedures is given here for clarity. The field measurements were obtained with temperature and humidity controlled nephelometry and aerosol particle filter sampling.

Temperature and humidity controlled nephelometry makes use of the hygroscopic and thermal behavior of the aerosols and corresponding changes in σ_{sp}, with changes in temperature and humidity, to assess the chemical nature of the ambient aerosol components. Controlled humidity nephelometry was first conceived by Pilat and Charlson (1966) and later developed and improved to include thermal processing by Larson et al. (1982) and Rood et al. (1987a). The innovative nature of the procedure relied upon the fact, that it provided the capability for in situ study of ambient aerosols, allowing the analysis of volatile and reactive species in the aerosol particles that may not be accurately collected and analyzed solely from filter or impactor samples.

The identification of the chemical species with temperature and humidity controlled nephelometry is based on calibration of the instrumentation with known compounds. The "signatures" of these compounds are recorded as changes in σ_{sp} with changes in temperature and/or humidity. These changes are caused by the thermal decomposition/volatilization of solute mass with increasing temperature and are also related to the

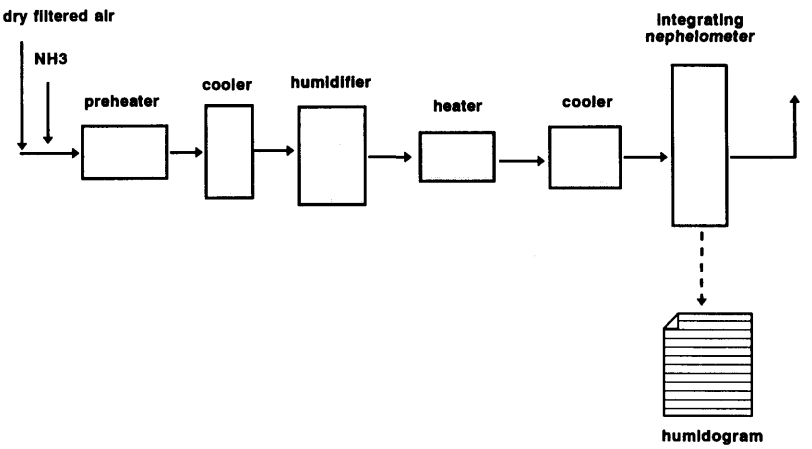

Fig. 1. Schematic of the temperature and humidity control system for in situ rapid response detection of ambient aerosol (Rood et al., 1987b).

hygroscopic properties of the particles. The effects of controlling the aerosol sample's temperature and relative humidity has been characterized experimentally with known inorganic salts such as $(NH_4)_2SO_4$, Na_2SO_4 and NH_4NO_3. These results have been described and discussed in detail by Rood et al. (1985; 1987a and b). The deliquescence humidity for reagent grade $(NH_4)_2SO_4$ has been measured in the laboratory and in the field as a test aerosol with the controlled relative humidity nephelometer. The measured deliquescence humidity for $(NH_4)_2SO_4$ is $80\% \pm 0.5\%$ relative humidity. Wishaw and Stokes (1954) report the deliquescence humidity for $(NH_4)_2SO_4$ at 79.96% relative humidity. Other reported values for the deliquescence humidity of suspended $(NH_4)_2SO_4$ particles range from 79.5 to 81% relative humidity (Tang 1980; Cohen et al., 1987).

Atmospheric aerosol was sampled at a flow rate of 300 l/min. The sample stream was first diluted with dry air to reduce its relative humidity to less than 35% and then passed through a cyclone with 50% collection efficiency at a particle diameter of 2.0 μm. The particles of interest in this study are accumulation mode particles with diameters in the 0.1 to 2 μm range. A portion of the diluted stream flowed through the system as shown in Fig. 1. The purpose of the instrument sequence shown was to detect σ_{sp} for a series of temperature and relative humidity conditions. First the aerosol was optionally preheated. The effect of preheating was to dry the aerosol and/or to volatilize solutes, so that the identification of the remaining refractive compounds in the aerosol particles is facilitated. Given that identification can depend on the occurrence of deliquescence, the increased temperature was also aimed to remove NH_4NO_3 from the particles, whose deliquescent behavior has been shown difficult to observe experimentally (Tang, 1980) and therefore its presence could inhibit observable occurrence of deliquescence.

The aerosol then passed through regions of controlled humidity and temperature conditions. Humidification took place in a wetted wall humidifier. The sample was subsequently heated to 60°C for 0.1 s, to decrease relative humidity to less than 20%, before rapidly cooling the sample to achieve a controlled relative humidity ranging between about 50 and 85% as the sample entered the integrating nephelometer. Results are provided as graphs describing the normalized σ_{sp} values as a function of relative humidity (humidograms). Typical humidograms of the sampled atmospheric aerosol are presented in Fig. 2. There was a clear change in response of σ_{sp} to increasing relative humidity conditions, when the aerosol was preheated to 190°C with $NH_{3(gas)}$ injection. The addition of $NH_{3(gas)}$ was meant to chemically

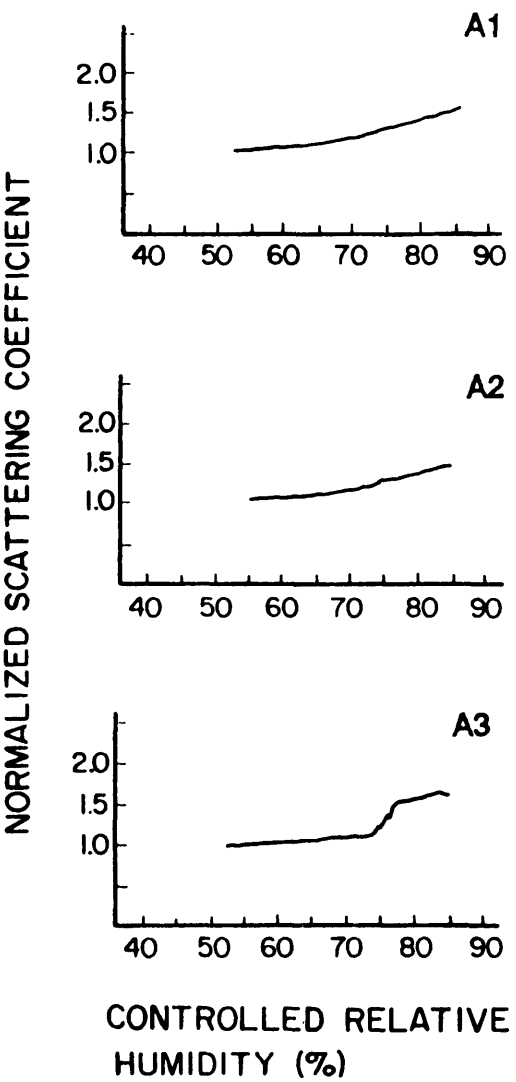

Fig. 2. Humidograms of typical ambient atmospheric aerosols: humidograms without preheating (A1), with preheating to 100°C (A2) and with preheating to 190°C with $NH_{3(gas)}$ injection (A3) (Rood et al., 1987b).

neutralize the aerosol and make up for NH_4^+ mass loss incurred during thermal treatment (Rood et al., 1987a). The abrupt change in σ_{sp} with a small change in relative humidity is interpreted as deliquescence. There was never more than one step change in σ_{sp} observed with the thermally treated and chemically neutralized aerosol. The minimum detectable change was 2% due to electronic noise from the instrumentation (Rood et al., 1987a).

Aerosol filter samples were taken simultaneously by drawing ambient aerosol through a cyclone, a nitric acid denuder and then a 25 mm diameter nylon filter at a flow rate of 10 l/min. Duration of filter sampling ranged from 4 to 9 h.

4. Summary of field results

The aerosols sampled in Riverside displayed deliquescent behavior after heating to 190°C with $NH_{3(gas)}$ injection, at relative humidities between 74 and 79%. These values are close to but less than the deliquescence humidity of $(NH_4)_2SO_4$. The fact that measured deliquescence humidities were lower than the one corresponding to pure $(NH_4)_2SO_4$ suggests the presence of other refractory soluble materials existing in the aerosol. Collected supplemental filter data show that cations other than NH_4^+ were also present with Na^+ existing in significant quantities. Given (i) the larger size of NaCl (typically $> 2\ \mu m$ which was the cuttoff for the sampled aerosol particle sizes), (ii) the deliquescence humidity for NaCl is near 75%, which is lower than recorded in most of the cases and (iii) the highly refractory nature of Na_2SO_4, the assumption is made that all Na^+ exists as Na_2SO_4 with the balance of SO_4^{2-} existing as $(NH_4)_2SO_4$. The percent by mass quantities of Na_2SO_4 and $(NH_4)_2SO_4$ based on SO_4^{2-} ion measurements and the assumption mentioned above are shown in Table 1 (columns 1 and 2). Also, presented in Table 1 is the mass fraction, y, of Na_2SO_4 (column 3) and the field measured deliquescence humidities (column 6).

Table 1. *Concentrations of $(NH_4)_2SO_4$ and Na_2SO_4 on a dry basis and at saturation and deliquescence humidities measured in the field*

Na_2SO_4 dry (% by mass)	$(NH_4)_2SO_4$ dry (% by mass)	mass fraction (y)[a] of Na_2SO_4	Na_2SO_4 saturated (% by mass of solution)[b]	$(NH_4)_2SO_4$ saturated (% by mass of solution)[b]	Field measured deliquescence humidity (%)
(1)	(2)	(3)	(4)	(5)	(6)
6.2	93.8	0.062	2.81	41.40	79
5.3	94.7	0.053	2.50	41.50	77
13.9	86.1	0.139	6.50	39.00	77
10.9	89.1	0.109	5.20	39.80	76
5.6	94.4	0.056	2.44	41.47	76
5.3	94.7	0.053	2.50	41.50	78
12.9	87.1	0.129	6.25	38.26	77
12.5	87.5	0.125	5.56	39.46	76
9.4	90.6	0.094	4.38	40.33	75
14.6	85.4	0.146	6.87	38.79	75
17.4	82.6	0.174	8.12	38.46	78
14.5	85.5	0.145	6.76	38.86	75
17.1	82.9	0.171	8.06	38.46	75
10.5	89.5	0.105	5.00	40.13	75
13.5	86.5	0.135	6.25	38.80	75
4.0	96.0	0.040	1.88	41.81	74
7.4	92.6	0.074	3.19	40.80	75
1.8	98.2	0.018	1.25	42.21	75
14.9	85.1	0.149	6.88	38.80	77
15.8	84.2	0.158	7.50	38.46	77

[a] $y = [Na_2SO_4]/\{[(NH_4)_2SO_4] + [Na_2SO_4]\}$, where the concentrations are expressed as % by mass.
[b] From the phase diagram.

5. Estimation of the deliquescence humidities from the phase diagram of the $(NH_4)_2SO_4$-Na_2SO_4-H_2O system

In this section, the deliquescence humidities for the solute mixtures, observed in the field, are estimated from the phase diagram for the $(NH_4)_2SO_4$-Na_2SO_4-H_2O system. As previously mentioned, the deliquescence humidity for pure $(NH_4)_2SO_4$ is 79.96% (Wishaw and Stokes, 1954), for $Na_2SO_4 \cdot 10H_2O$, which is the thermodynamically stable state in bulk solution, at temperatures between -16 and 26.5°C the deliquescence humidity is 93.61% (Goldberg, 1981; Rard and Miller, 1981). Experimental and modeled deliquescence humidities for suspended Na_2SO_4 particles at temperatures in the 20 to 25°C range are between 84.2 and 86.5%, (Tang and Munkelwitz, 1992; Cohen et al., 1987), corresponding to anhydrous Na_2SO_4.

The data for the phase diagram of the $(NH_4)_2SO_4$-Na_2SO_4-H_2O system at 25°C are provided by Freeth (1924). The examined system is complicated because of the existence of the double salt $NaNH_4SO_4 \cdot 2H_2O$ and the existence of $Na_2SO_4 \cdot 10H_2O$ as the stable Na_2SO_4 form in bulk solution at 25°C. In addition, the compounds formed by Na^+, NH_4^+, SO_4^{2-} and H_2O partition themselves depending on the presence of other solutes and temperature (Fig. 3).

The phase diagram shown in Fig. 4 is for an isobaric and isothermal system. Values along the abscissa and ordinate correspond to percent by mass of Na_2SO_4 and $(NH_4)_2SO_4$ in solution, respectively. The origin (0, 0) corresponds to 100% $H_2O_{(liquid)}$. The diagonal line HF represents the relative composition of the dry solute. Line ABCD is the solubility line corresponding to the saturated solution and separates the homogeneous liquid-only phase region from the regions that include at least one solid phase. The dotted lines represent the borders between phase regions (e.g., 1, 2, 3) where transitions in the composition of solute will occur when crossing from one region to another. Point A corresponds to the saturated solution of pure $(NH_4)_2SO_4$. Point D to the saturated solution of pure Na_2SO_4. Points B and C are the eutectic points for the $(NH_4)_2SO_4$-Na_2SO_4-H_2O system.

The dashed lines within region L of the phase

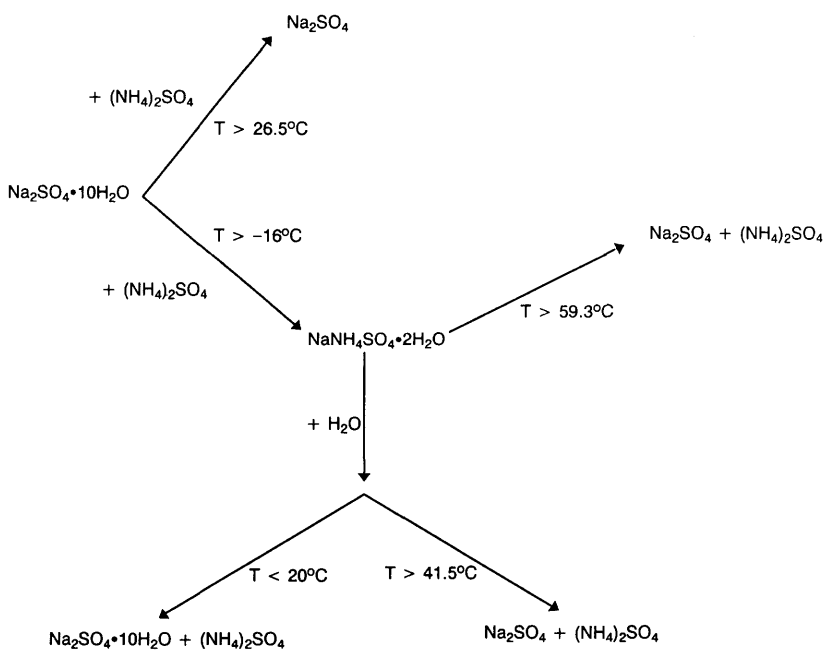

Fig. 3. Schematic of the partitioning of compounds in the $(NH_4)_2SO_4$-Na_2SO_4-H_2O system (according to Dawson, 1918).

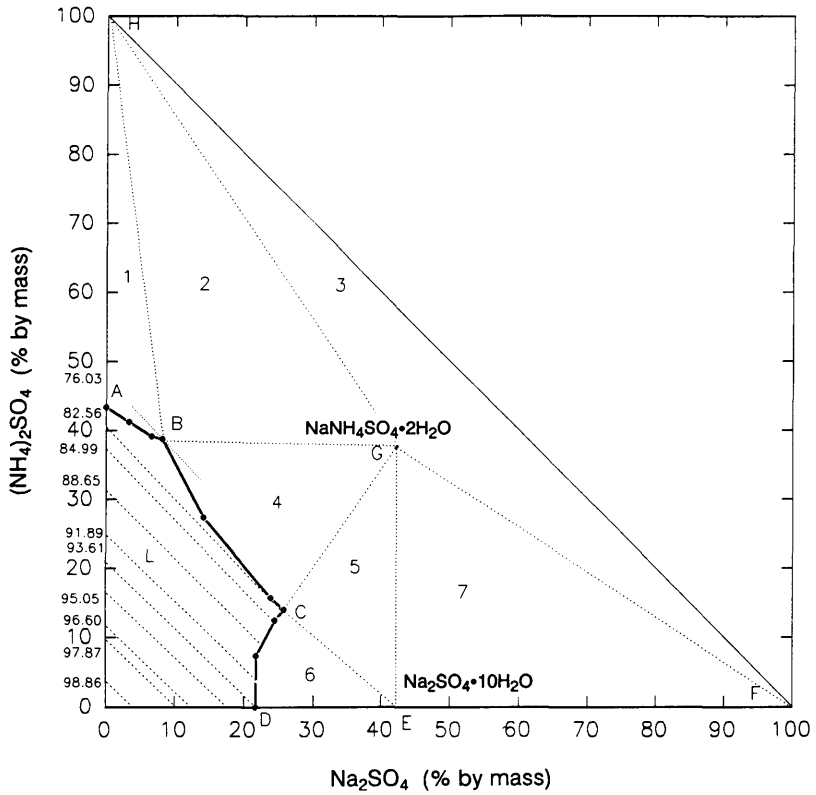

Fig. 4. Phase diagram and water activity lines for the $(NH_4)_2SO_4$-Na_2SO_4-H_2O system at 25°C (data from Freeth, 1924). L: liquid (subsaturated solution); 1: $(NH_4)_2SO_4$ and saturated liquid solution; 2: $(NH_4)_2SO_4$, $NaNH_4SO_4 \cdot 2H_2O$ and liquid of composition at B; 3: $NaNH_4SO_4 \cdot 2H_2O$, $(NH_4)_2SO_4$ and Na_2SO_4; 4: $NaNH_4SO_4 \cdot 2H_2O$ and saturated liquid solution; 5: $NaNH_4SO_4 \cdot 2H_2O$, $Na_2SO_4 \cdot 10H_2O$ and liquid of composition at C; 6: $Na_2SO_4 \cdot 10H_2O$ and saturated liquid solution; 7: $Na_2SO_4 \cdot 10H_2O$, $NaNH_4SO_4 \cdot 2H_2O$ and Na_2SO_4.

diagram represent lines of constant α_w. The terms water activity, α_w, and relative humidity are used interchangeably here. α_w, assuming subsaturated $H_2O_{(gas)}$ concentration and insignificant Kelvin effect, is given as: $\alpha_w = p_i/p_o$, where p_i is the vapor pressure over a solution and p_o the vapor pressure over pure water at the same temperature. Under the assumption of equilibrium of water between the gas and liquid phases, α_w is equal to relative humidity and at solute saturation, equal to the deliquescence humidity for that solute.

The straight dashed lines within region L of the phase diagram (Fig. 4) connect the mass concentrations of single electrolyte solutions of $(NH_4)_2SO_4$ and Na_2SO_4 with the same value for α_w. α_w lines beyond the saturation limits for the single solute solutions, found in the literature (Goldberg, 1981; Wishaw and Stokes, 1954), were determined with extrapolation, according to the method suggested by Tang (1976). More recently Cohen et al. (1987) have reported α_w values for single pure particles of $(NH_4)_2SO_4$ or Na_2SO_4 observed in an electrodynamic particle balance. Results from Tang's (1978) extrapolation method and Cohen et al.'s (1987) measurements are in agreement at the concentrations of interest in this work. Because of the lack of more available data, α_w lines are assumed to be straight lines.

An expanded version of the lower left part of Fig. 4 is presented in Fig. 5. The results obtained from the ambient filter samples are also included, displayed at their respective saturation concentrations along the solubility line, as open squares. The saturation concentrations were determined by the

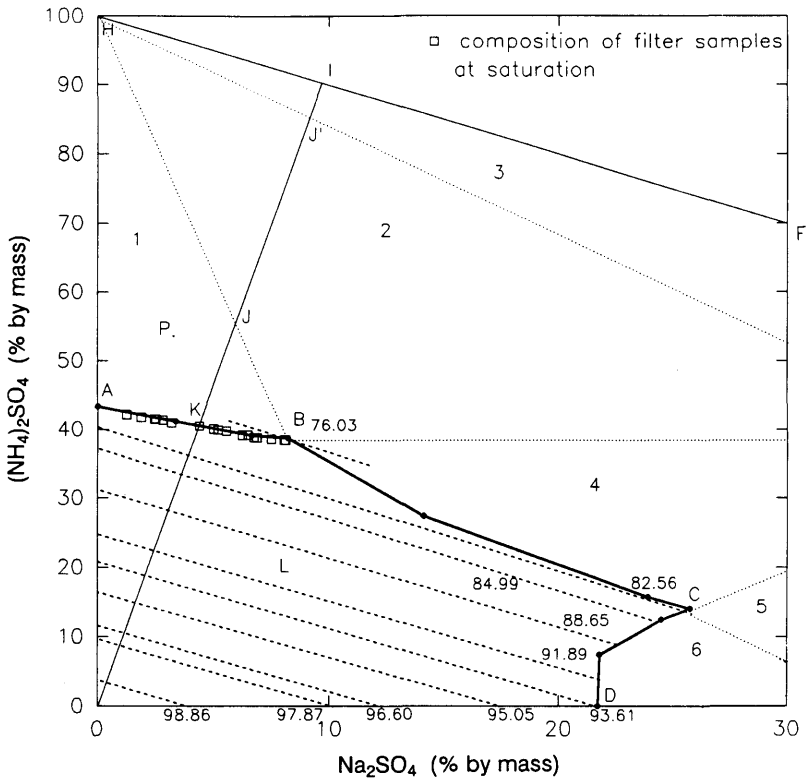

Fig. 5. Expanded view of solubility and water activity lines and observed mixtures at saturation for the $(NH_4)_2SO_4$-Na_2SO_4-H_2O system at 25°C.

intersection of the solubility line (line AB) with lines connecting the origin of the plot (0, 0) with the respective dry composition along line HF, as described in Table 1 (columns 1 and 2). That is, if the filter sampling gives a dry mixture at composition represented by I, then the composition of the corresponding saturated solution is represented by *K*. The values for the concentrations at saturation, determined from Fig. 5, are shown in Table 1 (columns 4 and 5). Moving from I to (0, 0) describes the transitions of the mixture as it takes up $H_2O_{(liquid)}$. From the dry solid phase it passes through the three phase region 3 to the three phase region 2, to the two phase region 1 to the one phase (only liquid) region L.

The Gibbs phase rule states that $F = C - P + 2$. F is the variance of the system that is, the number of independently variant intensive quantities whose values must be fixed to determine the state of the system, C is the number of components, P is the number of phases present at equilibrium in the system (Adamson, 1986). The $(NH_4)_2SO_4$-Na_2SO_4-H_2O system consists of three independently variable components and the phase rule, for $C = 3$ gives $F = 5 - P$. For constant total pressure and temperature, the system loses two degrees of freedom and $F = 3 - P$. That is the maximum number of co-existing phases is 3, which is verified with the phase diagram. As the dry mixture at I (Fig. 5), takes up $H_2O_{(liquid)}$ it passes through regions 3 and 2, with no degrees of freedom. For constant total pressure and temperature, continued $H_2O_{(liquid)}$ uptake changes the relative amounts but not the compositions of the phases present within regions 3 and 2. In region 2, after point J' is reached, $H_2O_{(liquid)}$ not existing as a hydrate forms a saturated liquid phase of constant composition.

Table 2. *Estimated deliquescence humidities for pure solute saturation points and eutonics*

Point on solubility line	Na_2SO_4 saturated (% by mass)	$(NH_4)_2SO_4$ saturated (% by mass)	Na_2SO_4 mass fraction $y^{(a)}$	α_w from the phase diagram (%)	estimated α_w from the osmotic coefficients (%)	estimated α_w from electrodynamic particle balance measurements (%)
(1)	(2)	(3)	(4)	(5)	(6)	(7)
A	0.00	43.40	0	80.08	80.08	79.22
B	7.70	38.70	0.165	76.03 □	76.26 ○	75.36 ◇
C	25.76	14.10	0.646	81.53	81.77	80.56
D	21.71	0.00	1	93.61	93.62	93.92

(a) $y = [Na_2SO_4]/\{[(NH_4)_2SO_4] + [Na_2SO_4]\}$, where the concentrations are expressed as % by mass.
□ (DH1)ph ○ (DH1)th ◇ (DH1)co.

Similarly, for a point along the equilibrium line HB, between regions/states 1 and 2, only the relative proportion of the solid to liquid phase changes. For a certain point on line HB, say J, the ratio JH/JB gives the mass ratio of the liquid to solid phases where the liquid phase has the composition at the eutectic point B and the solid is pure $(NH_4)_2SO_4$. Because of restrictions resulting from the phase rule, the vapor pressure of $H_2O_{(gas)}$ that determines α_w remains constant along line HB corresponding to the α_w at the eutectic point B (Adamson, 1986; Tang et al., 1978). At point J, all $NaNH_4SO_4 \cdot 2H_2O$ dissolves. This dissolution coincides with the onset of the aerosol particle growth corresponding to α_w (DH1)ph. Below point J, the vapor pressure of $H_2O_{(gas)}$ increases, as the concentration of solid in the liquid phase decreases. This is justified by the fact that in region. 1 only one liquid and one solid phase exist and the system gains one degree of freedom. Therefore, the vapor pressure of $H_2O_{(gas)}$ varies in region 1. Continued water uptake changes the composition of the liquid phase. For a point P in region 1, α_w is given by the corresponding α_w along the solubility line, at the point where HP crosses the solubility line AB. At a point K, along line AB, all remaining pure solid $(NH_4)_2SO_4$ dissolves and a saturated liquid phase forms.

A step change in mass and in σ_{sp} is expected at point J, as immediately past point J the change in α_w corresponds to a change in mass of $H_2O_{(liquid)}$. To display this, the Zdanovskii–Stokes–Robinson (ZSR) relationship (Wexler and Seinfeld, 1991) is considered. ZSR gives the mass of $H_2O_{(liquid)}$ in the aerosol particles as follows:

$$W = \sum_i (M_i/m_{i,o(\alpha_w)}), \qquad (1)$$

where W is the mass of $H_2O_{(liquid)}$ in the aerosol in kg per m^3 of air, M_i is the number of moles of solute i per m^3 of air and $m_{i,o(\alpha_w)}$ is the molality (mole/kg) of a pure solution of solute i at α_w. Therefore, for a given M_i, $m_{i,o(\alpha_w)}$ will decrease as α_w increases. For the $(NH_4)_2SO_4$-Na_2SO_4-H_2O system, past point J and towards point K, both the terms of the summation in eq. (1), corresponding to each Na_2SO_4 and $(NH_4)_2SO_4$ component, increase with increasing α_w until point K.

Table 3. *Estimated deliquescence humidities*

Na_2SO_4 mass fraction $y^{(a)}$	estimated (DH2)ph (%)	estimated (DH2)th (%)	estimated (DH2)co (%)
(1)	(2)	(3)	(4)
0.062	78.72	79.04	78.16
0.053	78.93	79.24	78.40
0.139	77.08	77.16	76.46
0.109	77.72	77.88	77.14
0.056	79.04	79.29	78.47
0.053	78.93	79.19	78.41
0.129	77.08	77.46	77.51
0.125	77.72	77.62	77.02
0.094	77.80	78.21	77.51
0.146	76.92	77.17	76.26
0.174	76.20	76.01	75.12
0.145	76.92	77.22	76.30
0.171	76.20	76.02	75.20
0.105	77.72	77.92	77.04
0.135	77.44	77.56	76.93
0.040	78.93	79.64	78.76
0.074	78.72	79.04	78.29
0.018	79.34	79.91	79.09
0.149	77.35	77.14	76.20
0.158	76.45	76.66	75.87

(a) $y = [Na_2SO_4]/\{[(NH_4)_2SO_4] + [Na_2SO_4]\}$, where the concentrations are expressed as % by mass.

At point K, complete dissolution of $(NH_4)_2SO_4$ occurs and a homogeneous solution is formed. A change in slope rather than a step change in mass is expected at K based on the phase diagram. The corresponding value for α_w is denoted as (DH2)ph.

Given the composition of the aerosol particles from the filter data (dry mixtures), all the field measured data at saturation (no solid phase present) lie along line AB. Therefore, all lines connecting the origin with the dry composition will cross line HB. Therefore, for all samples the first deliquescence point (DH1)ph occurs at a relative humidity equal to 76.03%, which is α_w of the eutectic point B. The relative humidities where all the $(NH_4)_2SO_4$ completely dissolves, (DH2)ph, is given by α_w values corresponding to the saturated compositions along line AB (Fig. 5). The values of (DH1)ph and (DH2)ph read from the phase diagram are shown in Table 2 (column 5) and Table 3 (column 2), respectively.

6. Estimation of the deliquescence humidities from thermodynamic modeling for the $(NH_4)_2SO_4$-Na_2SO_4-H_2O system

6.1. *Estimation of the deliquescence humidities based on measurements of the osmotic coefficients of subsaturated and saturated solutions of $(NH_4)_2SO_4$ and Na_2SO_4*

An alternate way to estimate α_w is by using the molal osmotic coefficient ϕ, which is defined by:

$$\phi = -1000(G - G_o)/(RTvm\,MW_1), \tag{2}$$

where G is the partial molal Gibbs energy of solvent in solution, G_o is the standard molal Gibbs energy of the solvent, R is the gas constant, T is the temperature, m is the molality of the solute, MW_1 the molecular weight of the solvent and v is the number of ions a molecule of the solute can form (Hamer and Wu, 1972).

For the case of a single electrolyte dissociating into v ions and on a molal basis the osmotic coefficient is expressed as:

$$\phi = -(1000/vm\,MW_1)\ln(\alpha_w). \tag{3}$$

Therefore from eq. (3), if ϕ is known α_w of an aqueous solution of a single solute can be estimated by eq. 4 (Hamer and Wu, 1972):

$$\ln \alpha_w = -(\phi vm/55.55). \tag{4}$$

α_w values differ between pure and mixed solutions for a given ionic strength. In addition, the Debye–Hückel approximation (Appendix) for activity coefficients is not valid with atmospheric aerosols given atmospheric aerosols exist in highly concentrated solutions. Expressions describing α_w for highly concentrated solutions with more than one electrolyte have been developed (Kusik and Meissner, 1978). In these expressions, all ions in solution are identified and by convention, the cations are characterized by consecutive odd numbers and the anions by consecutive even numbers. The following expression is valid for the $(NH_4)_2SO_4$-Na_2SO_4-H_2O system:

$$\ln(\alpha_{wmix}) = X_1 Y_2 \ln(\alpha_{12}) + X_3 Y_2 \ln(\alpha_{32}). \tag{5}$$

In eq. (5), Na^+ is characterized by 1, NH_4^+ by 3 and SO_4^{2-} by 2. α_{12} and α_{32} represent α_w for solutions containing pure Na_2SO_4 and $(NH_4)_2SO_4$ respectively, at the ionic strength of the mixture. X_i and Y_i represent the cationic and anionic fractions for each component respectively, that is:

$$X_1 = \frac{I_1}{I_1 + I_3} = \frac{0.5m_1z_1^2}{0.5(m_1z_1^2 + m_3z_3^2)}, \tag{6}$$

$$X_3 = \frac{I_3}{I_1 + I_3} = \frac{0.5m_3z_3^2}{0.5(m_1z_1^2 + m_3z_3^2)}, \tag{7}$$

$$Y_2 = \frac{I_2}{I_2} = \frac{0.5m_2z_2^2}{0.5m_2z_2^2}, \tag{8}$$

where z represents the ion's valence, m the ion's molality (mole/1000 g water) and I is the ionic strength of the solution. Therefore, eq. (5) for the $(NH_4)_2SO_4$-Na_2SO_4-H_2O system becomes:

$$\ln(\alpha_{wmix}) = y^* \ln(\alpha_{12}) + (1 - y^*)\ln(\alpha_{32}), \tag{9}$$

where y^* is the mole fraction for Na_2SO_4 ($y^* = [Na_2SO_4]/\{[Na_2SO_4] + [(NH_4)_2SO_4]\}$).

α_{12} and α_{32} in expressions (5) and (9) can be determined from their respective osmotic coefficients. The expression for the osmotic coefficient, given in Hamer and Wu (1972) and Staples and Nuttall (1977), is:

$$\phi = 1 + \frac{A_1}{B^3 I}\left[-(1 + BI^{0.5}) + 2\ln(1 + BI^{0.5}) + \frac{1}{(1 + BI^{0.5})}\right] + \frac{1}{2}Cm + \frac{2}{3}Dm^2 + \frac{3}{4}Em^3 + \cdots, \tag{10}$$

where $A_1 = 2A$ for electrolytes with 1, 2 valence (e.g., Na_2SO_4 or $(NH_4)_2SO_4$), where A is the coefficient in the Debye–Hückel equation (Appendix). The other coefficients for Na_2SO_4 are provided by Goldberg (1981): $B = 1.215973148$, $C = -0.355728552$, $D = 0.082946556$, $E = -0.004869541$. The coefficients for $(NH_4)_2SO_4$ were obtained from Stelson and Seinfeld (1982) and Fang (1986): $B = 1.02$, $C = -0.08369$, $D = 0.007635$, $E = -0.0003307$, $F = 5.783 \times 10^{-6}$.

The estimated values of the deliquescence humidities, (DH1)th and (DH2)th, for the compositions corresponding to points A, B, C, and D of the solubility line (Fig. 5) as well as, for the observed compositions measured from filter samples are shown in Table 2 (column 6) and Table 3 (column 3), respectively.

6.2. *Estimation of the deliquescence humidities from electrodynamic particle balance measurements of the water activities of highly concentrated solutions of $(NH_4)_2SO_4$ and Na_2SO_4*

Alternatively, Cohen et al. (1987) have presented polynomial fits of α_{12} and α_{32} with molality, m, by combining experimental single particle measurements with bulk literature data. For pure Na_2SO_4 in $H_2O_{(liquid)}$:

$$\alpha_{12} = 1.0052 - 6.484 \times 10^{-2}m + 3.519 \times 10^{-2}m^2 - 1.319 \times 10^{-2}m^3 + 1.925 \times 10^{-3}m^4 - 1.224 \times 10^{-4}m^5 + 2.870 \times 10^{-6}m^6 \quad (11)$$

There are two expression suggested for pure $(NH_4)_2SO_4$ in $H_2O_{(liquid)}$ by Cohen et al. (1987):

(i) $$\alpha_{32} = 0.9968 - 2.969 \times 10^{-2}m + 1.753 \times 10^{-5}m^2 - 3.253 \times 10^{-4}m^3 + 3.571 \times 10^{-5}m^4 - 9.787 \times 10^{-7}m^5 \quad (12a)$$

and

(ii) $$\alpha_{32} = 1.0151 - 4.478 \times 10^{-2}m + 1.041 \times 10^{-3}m^2 - 8.258 \times 10^{-6}m^3. \quad (12b)$$

The mean of the two α_{32} values are used for the calculation of the α_{wmix} with eq. (9).

The estimated values of the deliquescence humidities, (DH1)co and (DH2)co, for the compositions corresponding to points A, B, C, and D of the solubility line (Fig. 5) as well as, for the observed compositions measured with filters are shown in Tables 2 (column 7) and 3 (column 4), respectively.

7. Comparison of deliquescence humidities measured in the field with deliquescence humidities estimated from laboratory measurements and thermodynamic modeling for the $(NH_4)_2SO_4$-Na_2SO_4-H_2O system

The values of the deliquescence humidities (DH) measured in the field relative to the values from the phase diagram or estimated from thermodynamic modeling, for the different Na_2SO_4 mass fractions are presented in Figs. 6–8. The dashed lines in the figures correspond to the first deliquescence humidity ((DH1)ph, (DH1)th or (DH1)co), corresponding to the α_{wmix} of the eutectic point B. The open triangles, filled circles and open diamonds correspond to the deliquescence humidities when all the $(NH_4)_2SO_4$ dissolves into solution as determined by the phase diagram, osmotic coefficients and electrodynamic particle balance measurements, respectively. The open squares are the deliquescence humidities measured

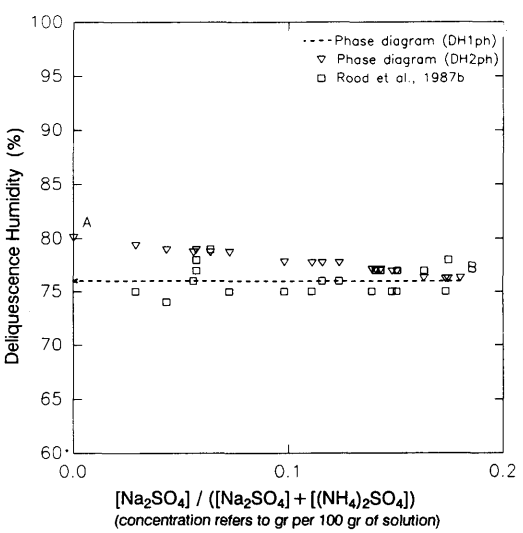

Fig. 6. Comparison between field measured and predicted deliquescence humidities from the phase diagram for the $(NH_4)_2SO_4$-Na_2SO_4-H_2O system.

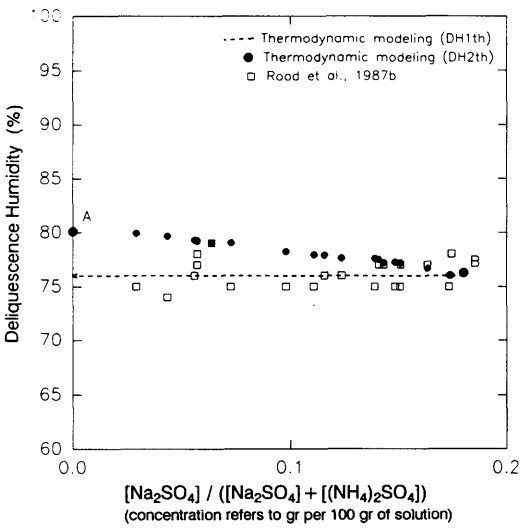

Fig. 7. Comparison between field measured and predicted deliquescence humidities from bulk measurements of the osmotic coefficients of aqueous solutions of pure $(NH_4)_2SO_4$ and Na_2SO_4 and thermodynamic modeling for the $(NH_4)_2SO_4$-Na_2SO_4-H_2O system.

in the field and correspond to the controlled relative humidities in the nephelometer when there was a large step change in σ_{sp} with a small change in relative humidity. All figures show that (DH2)ph, (DH2)th and (DH2)co are typically higher than the field measured values.

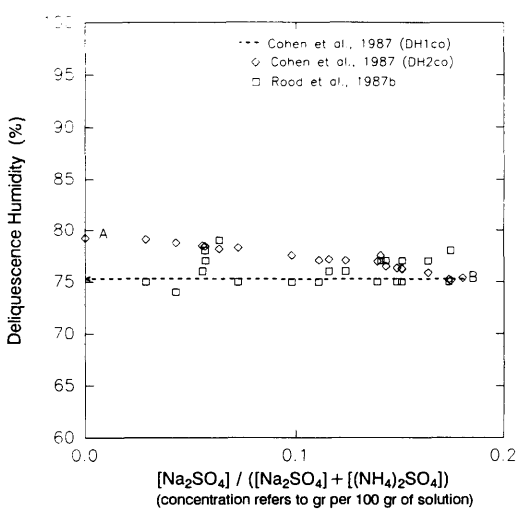

Fig. 8. Comparison between field measured and predicted deliquescence humidities from single pure particle laboratory measurements and thermodynamic modeling for the $(NH_4)_2SO_4$-Na_2SO_4-H_2O system.

Table 4. *Student t-test results*

compared pair	$\|t\|$	df, p	t-statistic
DH–(DH2)ph	1.405	38, 0.975	2.021
DH–(DH2)th	1.487	38, 0.975	2.021
DH–(DH2)co	0.880	38, 0.975	2.021
DH–(DH1)ph	0.235	19, 0.975	2.093
DH–(DH1)th	0.537	19, 0.975	2.093
DH–(DH1)co	2.483	19, 0.995	2.861
(DH2)ph–(DH2)th	0.190	38, 0.975	2.021
(DH2)th–(DH2)co	0.505	38, 0.975	2.021

Ho: mean (DH) = mean(DHi)n.

Student-t tests for the difference of means were performed for pairs of measured and estimated deliquescence humidities, as shown in Table 4. The tests resulted in no rejection of the null hypothesis at the 5% significance level, except for the comparison between DH and (DH1)co, where the confidence level should be increased to 99% for no rejection. The estimated t values support a closer correspondense between the field measurements and the estimated first deliquescence humidity points (DH1)ph and (DH1)th.

An estimation of the mean square roots of the squares of the differences between respective pairs give the results shown in Table 5. These estimations are provided because they give a measure of the relative differences between the compared

Table 5. *Comparison between measured and estimated pairs of deliquescence humidities*

Compared pairs of deliquescence humidities $(X_{i1} - X_{i2})$	mean square root of the squares of the differences[(a)]
DH–(DH2)ph	2.411
DH–(DH2)th	2.676
DH–(DH2)co	2.173
DH–(DH1)ph	1.336
DH–(DH1)th	1.344
DH–(DH1)co	1.536
(DH2)th–(DH2)co	0.810
(DH2)ph–(DH2)th	0.323

[(a)] $\sqrt{\sum_{i=1}^{n}((X_{i1} - X_{i2})^2/(n-1))}$, where 1 and 2 characterize each of the 2 groups of values that are compared and X_i represents the ith observation in each group (Clark and Hosking, 1986).

pairs. The field measurements are closer to the first deliquescence humidity point (DH1). Such result is a further indication that the observed large change in σ_{sp} with small change in relative humidity was correctly attributed to the change in phase and mass at DH1 which can be considered as the Mutual Deliquescence Humidity. Thereafter, σ_{sp} continued to increase in a smooth monotonic fashion, as the relative humidity increased for all humidograms.

The deviation between the field measurements (DH) with (DH1)ph, (DH1)th or (DH1)co can be due to the presence of other refractive soluble materials not accounted for in this analysis and the limitations inherent in the experimental procedure. A second step change in σ_{sp} could not have been detected if it was smaller than 2%, which is the estimated reliability of the σ_{sp} measurements. In addition, the present analysis of the $(NH_4)_2SO_4$-Na_2SO_4-H_2O system does not include the effect of the presence of an insoluble core such as soot (Hänel, 1976; Sloane, 1986) or of a possible coating with organic material (Gill et al., 1983; Hansson et al., 1990).

In a previous study (Sloane, 1986), the effect of aerosol composition on light scattering efficiency has been studied. In our study we have focused our interest on changes in σ_{sp} upon deliquescence, as a means for chemical compound identification. A combination of changes in scattering efficiency due to changing composition with shifts in deliquescence humidity could be used to this end. That will require further laboratory experiments with aerosol of known mixed composition. Such data are not currently available. Given this limitation, combined with further limitations in our current ability to assess exact ambient aerosol composition, we consider that the agreement of the field with empirical results of this analysis is satisfactory.

8. Summary and discussion

In this paper, in situ field measured aerosol data were considered. The ambient aerosol was heated with $NH_{3(gas)}$ injection and exposed to increasing relative humidity conditions to eliminate volatile particulate material and assess the composition of the more refractory particulate material.

The major component left after heating with $NH_{3(gas)}$ injection was believed to be $(NH_4)_2SO_4$. However, the observed deliquescence humidities were lower than the deliquescence humidity of pure $(NH_4)_2SO_4$. $(NH_4)_2SO_4$ was assumed to be internally mixed with Na_2SO_4. This hypothesis was tested by comparing the results from field measured deliquescence humidities with estimations of deliquescence humidities from the $(NH_4)_2SO_4$-Na_2SO_4-H_2O system, based on laboratory measurements and thermodynamic modeling. The analysis showed close correspondence between the field measurements and the estimated values of the deliquescence humidity. Therefore, it is shown that relatively small amounts of an ion (e.g., Na^+) can have a significant impact on the hygroscopic properties of aerosol particles that contain relatively large amounts of other ions such as SO_4^{2-} and NH_4^+. Such responses need to be included in the further evaluations of the hygroscopic properties of atmospheric aerosols.

Further research on atmospheric and laboratory aerosol chemistry needs to be performed to completely understand the hygroscopic properties of aerosol particles. The effect of hydrates on deliquescent behavior of atmospheric aerosols is not clearly described in the literature. For the specific $(NH_4)_2SO_4$-Na_2SO_4-H_2O system, it was seen that the thermodynamically stable states for Na_2SO_4 may not be the same between the bulk solutions and single droplets. Therefore, data obtained from bulk measurements and data obtained from single particle measurements should be compared very carefully. The thermodynamics of supersaturated solutions with respect to the anhydrous salt are also not exactly known. Such information will be useful for more accurate modeling of phase changes inside an aerosol droplet exposed to changing relative humidity conditions. The results presented here are considered good approximations within the current level of our understanding of atmospheric processes.

The results of this research strongly support the importance and potential of the combination of in situ optical methods with theoretical background for the assessment of ambient aerosol composition and behavior. This study demonstrates that rapid response in situ optical methods can be used for assessing chemical composition, in addition to providing the means for studying visibility

degradation and the effects of aerosol particles on the globe's energy balance (Charlson et al., 1992).

9. Acknowledgements

The authors would like to thank Anthony S. Wexler, Assistant Professor, University of Delaware, for useful conversations about the interpretation of the phase diagram. This research was performed under the auspices of the National Science Foundation under grant ATM-80-11395, and the National Oceanic and Atmospheric Administration under grant NA36GPO300.

10. Appendix

For dilute solutions the Debye–Hückel approximation gives the activity coefficients as follows:

$$-\log \gamma_i = (A\,|z_+ z_-|\,I^{1/2})/(1 + Ba_i I^{1/2}),$$

where γ_i is the activity coefficient. I is the ionic strength, z_+, z_- are the ion valences, a_i the hydrated ion radius. For electrolytes with 1, 2 valence such as Na_2SO_4 and $(NH_4)_2SO_4$, $A = 1.17625\ (kg^{1/2}\ mole^{-1/2})$ at 25°C and $B = 0.328 \times 10^{10}\ ((kg/mole)^{1/2}/m^{-1})$ at 25°C (Staples and Nuttall, 1977).

REFERENCES

Adamson, A. W. 1986. *A textbook of physical chemistry*, 3th edition. Academic Press College Division.

Cass, R. G. 1979. On the relationship between sulfate air quality and visibility with examples in Los Angeles. *Atmos. Environ.* **13**, 1069–1084.

Charlson, R. J. 1969. Atmospheric visibility related to aerosol mass concentration. *Environ. Sci. and Technol.* **3**, 913–918.

Charlson, R. J., Vanderpol, A. H., Covert, D. S., Waggoner, A. P. and Ahlquist, N. C. 1974. H_2SO_4/$(NH_4)_2SO_4$ background aerosol: optical detection in St. Louis region. *Atmos. Environ.* **8**, 1257–1267.

Charlson, R. J., Schwartz, S. E., Hales, J. M., Cess, R. D., Coakley, J. A. Jr., Hansen, J. E. and Hofmann, D. J. 1992. Climate forcing by anthropogenic aerosols. *Science* **255**, 423–430.

Clark, W. A. V. and Hosking, P. L. 1986. *Statistical methods for geographers*, New York, John Wiley & Sons, 233–261.

Cohen, M. D., Flagan, R. C. and Seinfeld, J. H. 1987. Studies of concentrated electrolyte solutions using the electrodynamic balance. 1. Water activities for single electrolyte solutions. *J. of Phys. Chem.* **91**, 4563–4574.

Covert, D. S., Charlson, R. J. and Ahlquist, N. C. 1972. A study of the relationship of chemical composition and humidity to light scattering by aerosols. *J. of Appl. Meteorol.* **11**, 968–976.

Covert, D. S., Waggoner, A. P., Weiss, R. E., Ahlquist, N. C. and Charlson, R. J. 1979. Atmospheric aerosols, humidity and visibility. In: *Character and origins of smog aerosols* (ed. G. M. Hidy). John Wiley & Sons, 559–581.

Dawson, H. M. 1918. The ternary system, sodium sulfate, ammonium sulfate and water. The utilisation of nitre cake for the production of ammonium sulfate. *J. of the Chem. Soc.* **113**, 675–688.

Fang, S. H. 1986. *Measurement and modeling of water activities for mixed aqueous solutions containing sodium, ammonium, nitrate and sulfate ions.* MS Thesis, University of Washington.

Freeth, F. A. 1924. Ternary and quaternary equilibria in the system: $NaClO_4$-$(NH_4)_2SO_4$-Na_2SO_4-H_2O at 60°C and 25°C. *Recueil des Travaux Chimiques des Pays-Bas* **XLIII**, 475–507.

Gill, P. S., Graedel, T. E. and Weschler, C. J. 1983. Organic films on atmospheric aerosol particles, fog droplets, cloud droplets, raindrops and snowflakes. *Rev. Geophys. Space Phys.* **21**, 903–920.

Goldberg, R. N. 1981. Evaluated activity and osmotic coefficients for aqueous solutions: Thirty six uni-bivalent electrolytes. *J. Phys. Chem. Ref. Data* **10**, 671–764.

Hamer, W. J. and Wu, Y. C. 1972. Osmotic coefficients and mean activity coefficients of uni-valent electrolytes in water at 25°C. *J. Phys. Chem. Ref. Data* **1**, 1047–1099.

Hänel, G. 1976. The properties of atmospheric aerosol particles as functions of the relative humidity at thermodynamic equilibrium with the surrounding moist air. *Advan. Geophys.* **19**, 73–188.

Hansson, H.-C., Wiedensohler, A., Rood, M. J. and Covert, D. S. 1990. Experimental determination of the hygroscopic properties of organically coated aerosol particles. *J. Aerosol Sci.* **21**, s241–s244.

Heintzenberg, J. 1989. Fine particles in the global troposphere. A review. *Tellus* **41B**, 149–160.

Kusik, C. L. and Meissner, H. P. 1978. Electrolyte activity coeffiecients in inorganic processing. *AIChE Symposium Series* **74**, 14–20.

Larson, T. V., Ahlquist, N. C., Weiss, R. E., Covert, D. C. and Waggoner, A. P. 1982. Chemical speciation of H_2SO_4-$(NH_4)_2SO_4$ particles using temperature and humidity controlled nephelometry. *Atmos. Environ.* **16**, 1587–1590.

Orr, C. Jr., Hurd, K. F. and Corbett, W. J. 1958. Aerosol size and relative humidity. *J. of Colloid Sci.* **13**, 472–482.

Pilat, M. J. and Charlson, R. J. 1966. Theoretical and optical studies of humidity effects on the size distribution of a hygroscopic aerosol. *J. Rech. Atmos.* **2**, 165–170.

Rard, J. A. and Miller, D. G. 1981. Isopiestic determina-

tion of the osmotic coefficients of aqueous Na_2SO_4, $MgSO_4$ and Na_2SO_4 and $MgSO_4$ at 25°C. *J. of Chem. Engin. Data* **26**, 33–38.

Rood, M. J., Larson, T. V., Covert, D. S. and Ahlquist, N. C. 1985. Measurement of laboratory and ambient aerosols with temperature and humidity controlled nephelometry. *Atmos. Environ.* **19**, 1181–1190.

Rood, M. J., Covert, D. S. and Larson, T. V. 1987a. Temperature and humidity controlled nephelometry: Improvements and calibration. *Aerosol Sci. Technol.* **7**, 57–65.

Rood, M. J., Covert, D. S. and Larson, T. V. 1987b. Hygroscopic properties of atmospheric aerosol in Riverside, California. *Tellus* **39B**, 383–397.

Sloane, C. S. 1986. Effect of composition on aerosol light scattering efficiencies. *Atmos. Environ.* **20**, 1025–1037.

Spann, J. F. and Richardson, C. B. 1985. Measurement of the water cycle in mixed ammonium acid sulfate particles. *Atmos. Environ.* **19**, 819–825.

Staples, B. R. and Nuttall, R. L. 1977. The activity and osmotic coefficients of aqueous Calcium Chloride at 298.15 K. *J. Phys. Chem. Ref. Data* **6**, 385–407.

Stelson, A. W. and Seinfeld, J. H. 1982. Thermodynamic prediction of the water activity, NH_4NO_3 dissociation constant, density and refractive index for the NH_4NO_3-$(NH_4)_2SO_4$-H_2O system at 25°C. *Atmos. Environ.* **16**, 2507–2514.

Tang, I. N. 1976. Phase transformation and growth of aerosol particles composed of mixed salts. *J. of Aerosol Sci.* **7**, 361–371.

Tang, I. N., Munkelwitz, H. R. and Davis, J. G. 1978. Aerosol growth studies-IV. Phase transformation of mixed salt aerosols in a moist atmosphere. *J. of Aerosol Sci.* **9**, 505–511.

Tang, I. N. 1980. Deliquescence properties and particle size change of hygroscopic aerosols. In: *Generation of aerosols and facilities for exposure experiments* (ed. K. Willeke). Ann Arbor Science, 153–167.

Tang, I. N., Wong, W. T. and Munkelwitz, H. R. 1981. The relative importance of atmospheric sulfates and nitrates in visibility reduction. *Atmos. Environ.* **15**, 2463–2471.

Tang, I. N. and Munkelwitz, H. R. 1992. Aerosol phase transformation and growth in the atmosphere. *DOE. Atmospheric Chemistry Program, Monthly Update* **3**, 4–9.

Waggoner, A. P., Weiss, R. E., Alhquist, N. C., Covert, D. S., Will, S. and Charlson, R. J. 1981. Optical characteristics of atmospheric aerosols. *Atmos. Environ.* **15**, 1891–1909.

Wexler, A. S. and Seinfeld, J. H. 1991. Second-generation inorganic aerosol model. *Atmos. Environ.* **25A**, 2731–2748.

Winkler, P. 1988. The growth of atmospheric aerosol particles with relative humidity. *Physica Scripta* **37**, 223–230.

Wishaw, B. F. and Stokes, R. H. 1954. Activities of aqueous ammonium sulfate solutions at 25°C. *Trans. Faraday Soc.* **50**, 952–954.